29th International Cosmic Ray Conference Pune (2005) **1**, 265–268

Development of the Fast Neutron Imaging Telescope (FNIT)

M.R. Moser[a], J.M. Ryan[b], U. Bravar[b], E.O. Flückiger[a], J.R. Macri[b] and M.L. McConnell[b]
(a) Physikalisches Institut, University of Bern, CH-3012 Bern, Switzerland
(b) Space Science Center & Physics Department, University of New Hampshire, Durham, NH 03824-3525, USA
Presenter: J.M. Ryan (Michael.Moser@phim.unibe.ch), swi-moser-M-abs2-sh16-poster

We report on the development of a next generation solar neutron telescope that is sensitive to neutrons in the energy range 3–100 MeV, optimized to study solar neutrons in the innermost heliosphere. The detection principle is based on multiple elastic neutron-proton scatterings in plastic scintillators. By reconstructing event locations and measuring the recoil proton energies, the direction and energy spectrum of the primary neutron flux can be determined. We present the results of recent laboratory efforts, and in combination with simulation data we outline the performance of the telescope under space conditions.

1. Introduction

Neutrons produced in high energy processes at the Sun can provide key information about the time evolution of the proton and ion spectra, since they uniquely sample a wide energy range, and their numbers reflect the composition of the high energy ions. When combined with γ-ray and ground-based cosmic ray data, one has indicators and measures of the proton and ion spectra from a few MeV up to GeV energies [1, 2].

Since solar neutrons do not survive in significant numbers, the energy range below some tens of MeV is not accessible at 1 AU. In order to observe the entire neutron spectrum down to $\sim$ 1 MeV, one has to operate optimized neutron spectrometers on missions to the innermost heliosphere, such as the NASA Solar Sentinel Mission that is currently in planning for a solar orbit between 0.3 and 0.7 AU.

2. Instrument Concept

The detection principle of the Fast Neutron Imaging Telescope (FNIT) [3] is based on fast neutron scattering off ambient protons (elastic n–p scattering) that obeys hard-sphere scattering physics. Plastic scintillator provides the proton target and is also an efficient detector of charged particles. The instrument is configured to locate n–p scatter sites within the detector using the scintillation light generated by the recoil protons. Multiple n–p scattering provides important kinematic information for the reconstruction of the direction and energy of the incident neutron and for rejecting background events.

Figure 1a schematically shows the kinematics of a neutron, whose incident direction is unknown, that undergoes three successive elastic n–p scatters. The recoil neutron directions are defined by the positions of the three scatter points that are registered together with the pulse height associated with each scatter and the time they occur. The direction of the recoil proton is not measured for any scatters since the range can be very short. If the neutron energy $E_{\rm n}$ is fully measured, the incident neutron direction lies on the mantle of a cone with half angle $\theta_{\rm n}$ around the first recoil neutron velocity vector. The superposition of many event circles, i.e., projections of the cone on the celestial sphere, provides the statistical information necessary to locate the source. Event circles from a point source intersect, whereas unrelated event circles, i.e., from background events, do not. This procedure is the same as was successfully used on the COMPTEL experiment to image MeV γ-ray and neutron sources [4, 5]. If a neutron only scatters twice, the energy measure is only a lower limit, i.e., the reconstructed half angle $\theta_{\rm n}$ will be systematically larger than its true value. Nevertheless, events can be rejected if the Sun lies outside the corresponding event circle.

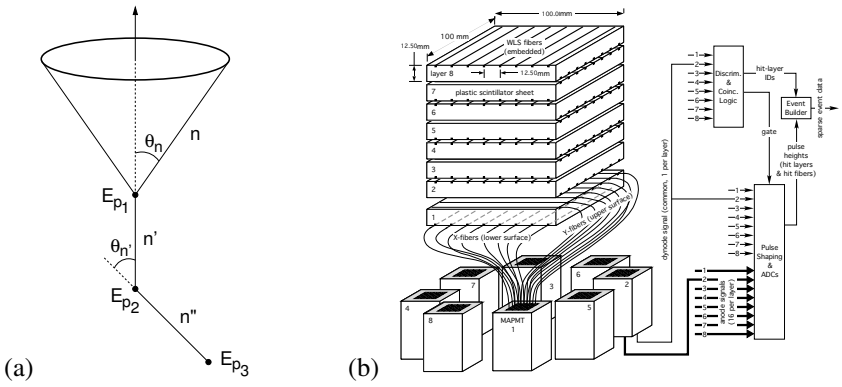

Figure 1. (a) Event circle reconstruction of a triple scatter event. (b) Schematic view of a possible implementation of the FNIT instrument. For details see text.

A possible implementation of a FNIT instrument employing this detection and imaging principle is illustrated in Figure 1b. Each detector layer is made from a plate of plastic scintillator. At the upper and lower face of each layer, wavelength shifting (WLS) fibers are bonded into grooves with regular pitch and orthogonal orientations. The clad WLS fibers of each layer guide the trapped portion of scintillation light to one pixel on the face of a multi-anode photomultiplier (MAPMT) for read out. These signals are used for the instrument trigger logic, the recoil energy measurement, and the reconstruction of the interaction location on each layer.

3. Laboratory Prototype

In the laboratory we evaluated the performance of the described concept with several prototype configurations having different dimensions, fiber pitches, and types of readout fibers. The detector configuration tested and reported here is 15 mm thick and has four parallel wavelength shifting (WLS) fibers per 15 mm pitch element connected to one MAPMT pixel. Below we present the response of this configuration for atmospheric muons and for a collimated radioactive source.

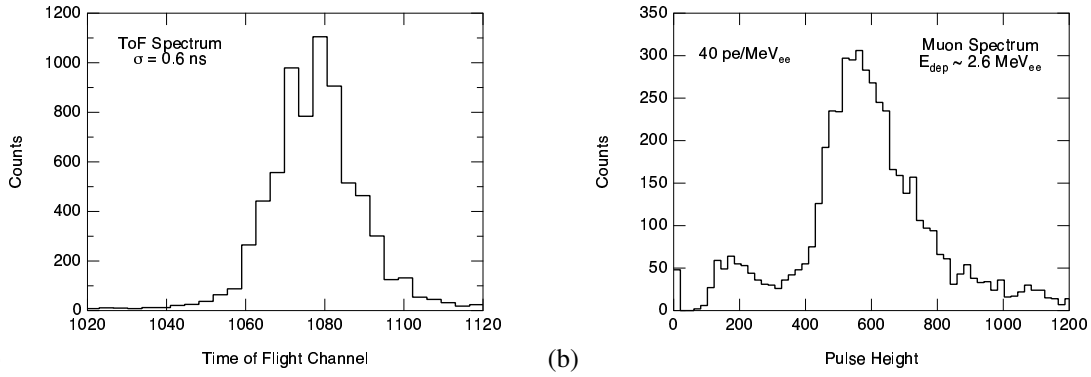

Figure 2. (a) Distribution of the TOF signal and (b) of the pulse height obtained from vertically propagating muons.

From coincidence measurements we determined the distribution of the time-of-flight (TOF) signal that is shown in Figure 2a. The determined 1σ resolution of the signal is 0.6 ns. The time information allows one to reject

Compton-scatter events induced by γ-rays. Furthermore, one is able to determine the direction of momentum of a neutron and thus to reject events by neutrons produced in the spacecraft. From these measurements the rejection efficiency is estimated to $\sim 90\%$ at 10 MeV, in agreement with instrument simulations.

Figure 2b shows the pulse height distribution induced by atmospheric muons in a 15 mm thick plate, corresponding to an energy deposit of 2.6 MeV electron equivalent (ee). From the peak value we calculated a yield of 40 photoelectrons per $\mathrm{MeV_{ee}}$. Because the scintillation photon yield for low-energy ions is lower than for electrons at the same energy, this corresponds to a neutron energy as low as ~ 1.5 MeV for single scatters, and ~ 3 MeV for double scatters. For this estimate we assume a threshold of 10 photoelectrons, however, it has to be chosen such that the location of interaction can be uniquely determined.

From the signal of a collimated $^{90}\mathrm{Sr}$ β-source we determined the horizontal spatial resolution as a function of position. Figure 3 shows the contour plots of the position distribution. The left plot (a) shows the distribution obtained by identification of the MAPMT pixel with the largest signal in each dimension. The narrower distribution in the right plot (b) is obtained by using an algorithm that also takes into account the signals of the neighboring pixels. Since the electrons enter the upper surface of the plate, the 1σ resolution in the Y-dimension is smaller ($0.53 \pm 0.02\,\mathrm{cm}$) than in the X-dimension ($1.28 \pm 0.03\,\mathrm{cm}$) because of the longer path of the photons through the scintillator. Compared to configurations with only one fiber per pitch element we achieve a lower energy threshold, and the horizontal position distribution became much more symmetric.

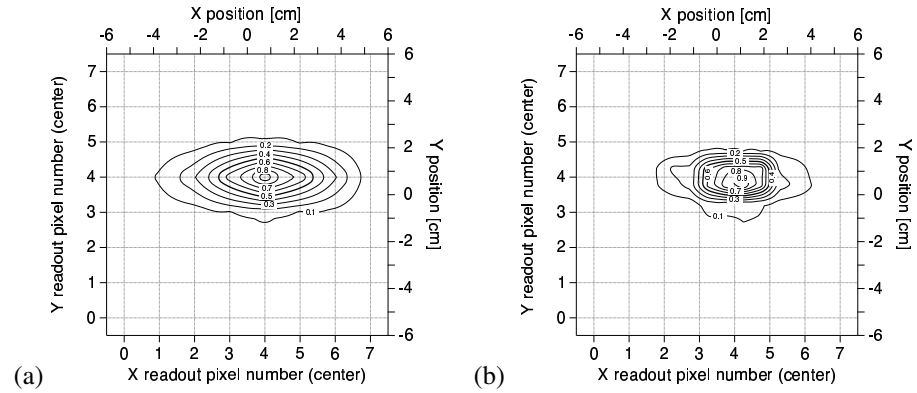

Figure 3. Contour plot of horizontal spatial resolution. In (a) the position is given by the MAPMT pixels measuring the largest signal in each dimension while in (b) also the signal of the neighboring pixels is taken into account.

4. Sensitivity

Figure 4a shows the calculated efficiency for a FNIT configuration with 10 tightly stacked $1.5 \times 10 \times 10\ \mathrm{cm}^3$ plastic scintillator layers. We computed the response of such a detector at a solar orbit of 0.3 AU for the X12 class solar flare on 15 June 1991 [6] during 30 minutes after the onset. The integral count rate above 3 MeV is shown in Figure 4. The instrument would detect ~ 2700 single and ~ 1700 double elastic n–p scatters below 10 MeV. In the energy range 10–100 MeV there would be ~ 3100 single and ~ 800 double elastic n–p scatters. As an estimate of the background neutron flux in a thick low-Z target we used the isotropized atmospheric albedo spectrum from Preszler et al. [7]. By folding this spectrum with the detector efficiency we obtained ~ 100 counts above 10 MeV during the event. The extrapolation of the background spectrum leads to ~ 100 counts in the interval 3–10 MeV. Therefore, neutrons from a flare of the magnitude of the 15 June 1991 event could be detected with a significance of $> 20\sigma$ in the double scatter mode above 10 MeV. Due to the high signal-to-noise ratio below 10 MeV the instrument is potentially able to discover low-energy neutrons from

weaker flares with softer accelerated ion spectra. However, detailed simulations of the background signal on a close solar orbit induced by γ-rays and SEPs still have to be performed.

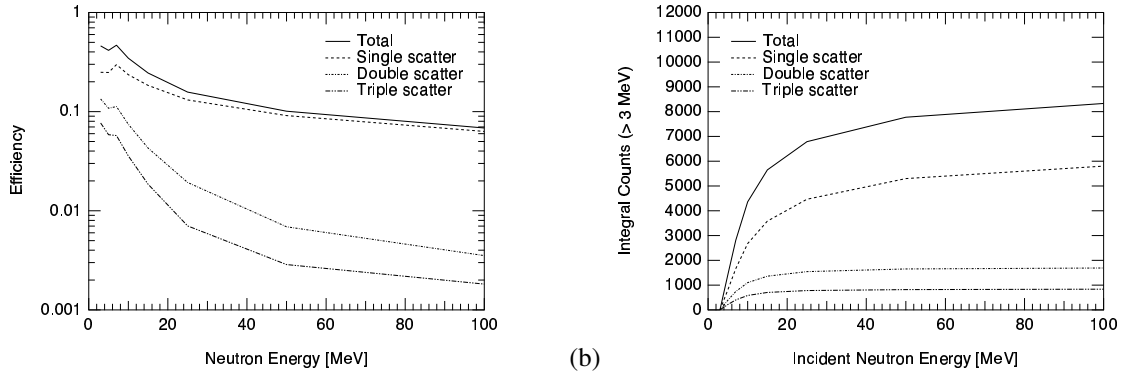

Figure 4. (a) Efficiencies of single, double, and triple n–p scattering for vertically incident neutrons on a configuration with ten $1.5 \times 10 \times 10$ cm^3 layers. (b) Calculated integral count rate > 3 MeV at 0.3 AU for the 15 June 1991 solar flare.

5. Further Development

The key to further improvements in the design of the detector is to increase the signal yield and thus to lower the energy threshold for which effective measurements of the energy deposit, timing, and position resolution can be made. New prototypes with optimized plate dimensions and fiber pitch incorporating better matched scintillation and wavelength shifting materials are under development. Another set of prototype detectors using liquid scintillator instead of plastic scintillators will be built and evaluated in the laboratory. Liquid scintillator detectors have an enhanced hydrogen to carbon ratio and thus are more efficient for multiple scatters. Furthermore, they offer the possibility of n–γ particle identification using pulse shape discrimination techniques. Upon establishment of a baseline detector configuration, laboratory studies will extend to multiple layer instrument prototypes, background rejection techniques, validation of the simulations for multiple interactions, and development of tools for instrument data analysis.

Acknowledgments

This research is supported in the United States by NASA's Living With a Star Targeted Research and Technology program (grant NAG5-13519), and in Switzerland by the Swiss National Science Foundation (grant 200020-105435/1).

References

[1] J.A. Lockwood, et al., *Solar Phys.*, **173**, 151 (1997).
[2] J.M. Ryan, et al., *Space Sci. Rev.*, **93**, 31 (2000).
[3] M.R. Moser, et al., *Adv. Space Res.*, in press (2005).
[4] J.M. Ryan, et al., in *Data Analysis in Astronomy IV*, Plenum Press New York, **59**, 261 (1992).
[5] H. de Boer, et al., in *Data Analysis in Astronomy IV*, Plenum Press New York, **59**, 241 (1992).
[6] H. Debrunner, et al., *Proc. 23rd Int. Cosmic Ray Conf.*, **3**, 115 (1993).
[7] A.M. Preszler, et al., *J. Geophys. Res.*, **81**, 4715 (1976).